

International Journal of Modern Physics: Conference Series
© World Scientific Publishing Company

FORMATION AND COLLIMATION OF RELATIVISTIC MHD JETS - SIMULATIONS AND RADIO MAPS

CHRISTIAN FENDT

*Max Planck Institute for Astronomy, Königstuhl 17,
69117 Heidelberg, Germany, fendt@mpia.de*

OLIVER PORTH

*Department of Applied Mathematics, The University of Leeds,
Leeds, LS2 9GT, United Kingdom*

SOMAYEH SHEIKHNEZAMI

*Max Planck Institute for Astronomy, Königstuhl 17,
69117 Heidelberg, Germany*

Received Day Month Year
Revised Day Month Year

We present results of magnetohydrodynamic (MHD) simulations of jet formation and propagation, discussing a variety of astrophysical setups. In the first approach we consider simulations of relativistic MHD jet formation, considering jets launched from the surface of a Keplerian disk, demonstrating numerically - for the first time - the self-collimating ability of relativistic MHD jets. We obtain Lorentz factors up to $\simeq 10$ while acquiring a high degree of collimation of about 1 degree. We then present synchrotron maps calculated from the intrinsic jet structure derived from the MHD jet formation simulation. We finally present (non-relativistic) MHD simulations of jet launching, treating the transition between accretion and ejection. These setups include a physical magnetic diffusivity which is essential for loading the accretion material onto the outflow. We find relatively high mass fluxes in the outflow, of the order of 20-40% of the accretion rate.

PACS numbers: 98.62.Mw, 95.30.Qd, 98.62.Nx, 98.38.Fs, 98.58.Fd

1. Introduction

Astrophysical jets are highly collimated streams of high-velocity. They are observed in a variety of astronomical sources, such as young stars, micro-quasars, or active galactic nuclei (AGN). The current understanding is that outflows are launched by *magnetohydrodynamic* (MHD) processes in the close vicinity of the central object - an accretion disk surrounding a protostar or a compact object^{1,2,3}. Besides the contribution of the disk wind to the overall jet flow, there is most probably also a contribution launched by the central object. In case of stellar sources, a stellar wind may contribute additional Poynting flux or pressure^{4,5,6}. In case of a central black hole, a central Poynting dominated spine jet may exist, driven by the Blandford-

2 Authors' Names

Znajek mechanism^{7,8}. Despite a huge effort, the details of all the physical processes involved are, however, not completely understood. Early treatments considered the stationary MHD equations, for example collimating magnetic jets in Kerr metric^{9,10,11}, but relativistic jet simulations are feasible since some decade^{12,13,14}.

Here we present results of axisymmetric MHD simulations investigating certain aspects of jet formation. We first present results for disk winds collimating into relativistic jets applying (special) relativistic MHD simulations from the surface of a Keplerian disk. We then apply a relativistic radiation transfer code to provide synchrotron maps of these outflows - applying the true internal structure derived by the numerical simulations. We finally present simulations of jet launching. These simulations treat the accretion and ejection process together, and therefore allow to derive the ejection efficiency of the accretion disk. As accretion is a (turbulently) diffusive process, these simulations apply an α -prescription of magnetic diffusivity. Since our code cannot treat diffusivity in the relativistic limit, these simulations are non-relativistic. For all our simulations we have applied the MHD code PLUTO¹⁵.

2. Relativistic MHD jets from accretion disks

Here we discuss (special) relativistic MHD simulations treating the formation of MHD jets from the surface of a disk. With *formation* we denote the acceleration and collimation of a disk wind into a high speed jet. In order to apply a Keplerian disk boundary condition for the jet, we have added Newtonian gravity to the special relativistic PLUTO code (see^{16,17}). Our standard setup involves a poloidal field considering a plasma- β between 0.001 and 1 at the inner disk radius and the poloidal field profile as a fixed-in-time boundary condition. The toroidal magnetic field is induced during the flow evolution and is floated into the boundary domain.

Figure 1 shows the relativistically distinct regimes of flow collimation. In the hydrodynamic regime upstream the Alfvén surface (I), gravity balances thermal and magnetic pressure, respectively the centrifugal force for cold jets. In the relativistic regime downstream the light surface (II), the poloidal magnetic pressure gradient imposes a collimating force against electric de-collimation. Electric forces ultimately overcome the classical magneto-centrifugal contribution. In the magneto-hydrodynamic regime downstream the Alfvén surface (III) the residuals of magnetic pinch and toroidal magnetic pressure gradient balance the centrifugal force¹⁶.

Figure 2 shows the typical result of a mildly relativistic jet with Lorentz factor of 1.5. The location of the magnetosonic surfaces is shown and also the light surface where $R_L(r, z) \equiv c/\Omega$. The asymptotic region of the relativistic jet enclosed by the light surface is the *truly relativistic part of the outflow*. This part of the outflow originates close to the inner edge of the accretion disk deep in the potential well where rotation is most rapid. We have also applied a model setup where we prescribe a higher Poynting flux by injecting plasma with a higher toroidal field strength (up to a factor 8) from the disk into the outflow. Depending on the Poynting flux injected, the resulting jet Lorentz factors reach number values between of 1.5 -

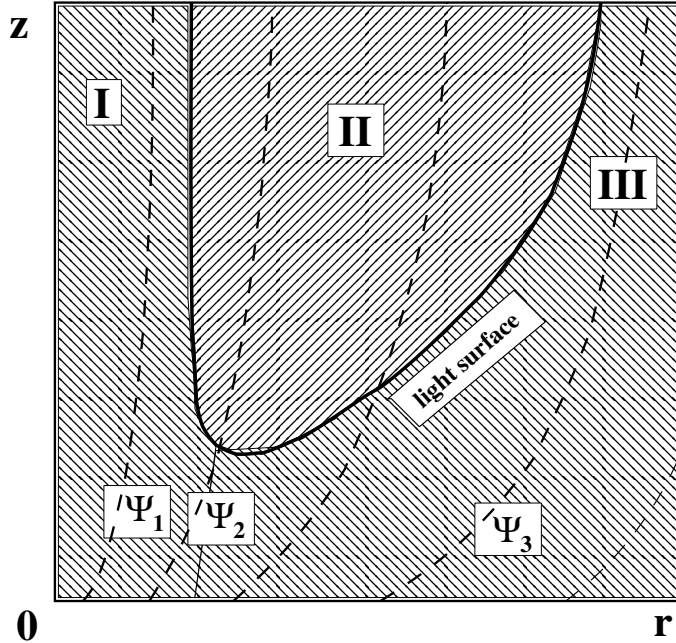


Fig. 1. The dynamical regimes of special relativistic disk-winds. Region I and III stay sub-relativistic, region II is relativistic, i.e. electric forces are not negligible. Figure taken from [16].

10. Typical jet opening angles for the relativistic part of the outflow are $1 - 7$ degrees, however, on the physical scales covered by the simulations of up to 6000^2 Schwarzschild radii the asymptotic jet is not jet fully accelerated or collimated.

We interpret our results as a numerical proof of MHD jet self-collimation. We have applied a modified outflow boundary condition, which is force-free concerning the Lorentz forces. Moreover, the poloidal magnetic field strength as well as the gas pressure decrease with axial distance from the jet axis. Therefore, no collimating forces are present from these terms, but only the tension force of the toroidal field. This is the first time that the predictions by Heavearts & Norman¹⁸ and Chiueh et al.¹⁹ of MHD jet self-collimation are proven by numerical simulations for relativistic jets. Note that we particularly calculate the force-equilibrium across the light surface and do *not* apply the conventional limit for asymptotic approximations of $r \gg r_L$. Further, there is no outer medium present which collimates the outflow.

3. Synchrotron maps of simulated MHD jets

Having derived a physically consistent distribution of the MHD variables by our numerical simulations - i.e. the jet magnetic field distribution, the density distribution, and the jet velocity - we may use this information to derive consistent radio synchrotron maps following a relativistic polarized radiation transfer within the jet. Since we have not included particle acceleration in the MHD model, additional as-

4 Authors' Names

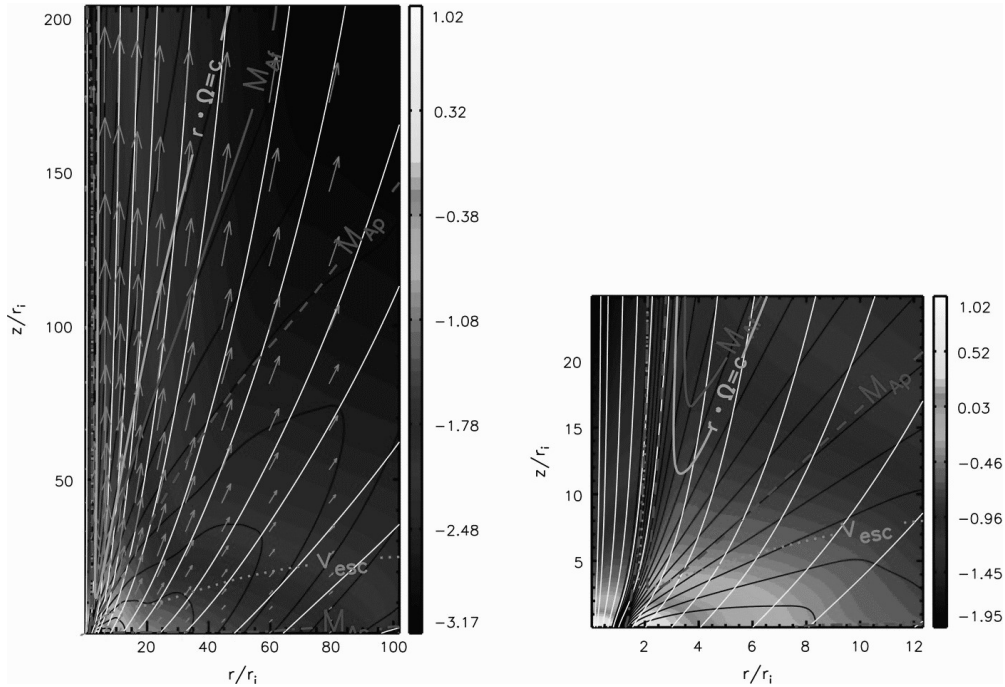


Fig. 2. Rest-frame density (grey colors, logarithmic) of the stationary flow. Shown are poloidal magnetic field lines (solid white), electric stream lines (solid black), characteristic MHD surfaces (various dot-dashed grey, labeled as M_{As} , M_{Ap} , M_{Ar}), the surface of escape velocity (dotted grey, labeled as V_{esc}), the light surface (solid grey, labeled as $r \cdot \Omega = c$). Arrows indicate the velocity field. The right figure is the enlarged central region, indicating the three regimes defined by the light surface. Figures taken from [16].

sumptions have to be made. We have tested three tracers for the power-law particle acceleration, i.e. density, thermal pressure, or magnetic energy density¹⁷. All tracers give a similar polarization structure, although the intensity distribution differs. Figure 3 shows the polarization degree and polarisation vectors for jet inclination 30, 20, and 10 degrees, emitted from regions with different comoving pitches B'_ϕ/B'_p .

4. Jet launching from accretion disks

We now show simulations treating the *launching* of the outflow - i.e. the transition from accretion to ejection. Accretion disk physics usually relies on (turbulent) magnetic diffusivity (unless a high-enough resolution is applied resolving the magneto-rotational instability). Only few relativistic codes are able to apply a physical magnetic resistivity (see e.g. [20]). In order to treat the diffusive MHD launching problem, we have therefore applied a non-relativistic approach^{21,22}.

Figure 4 shows results from our bipolar simulations. The simulations were run from a symmetric initial condition, apart from a hemispheric asymmetry in the

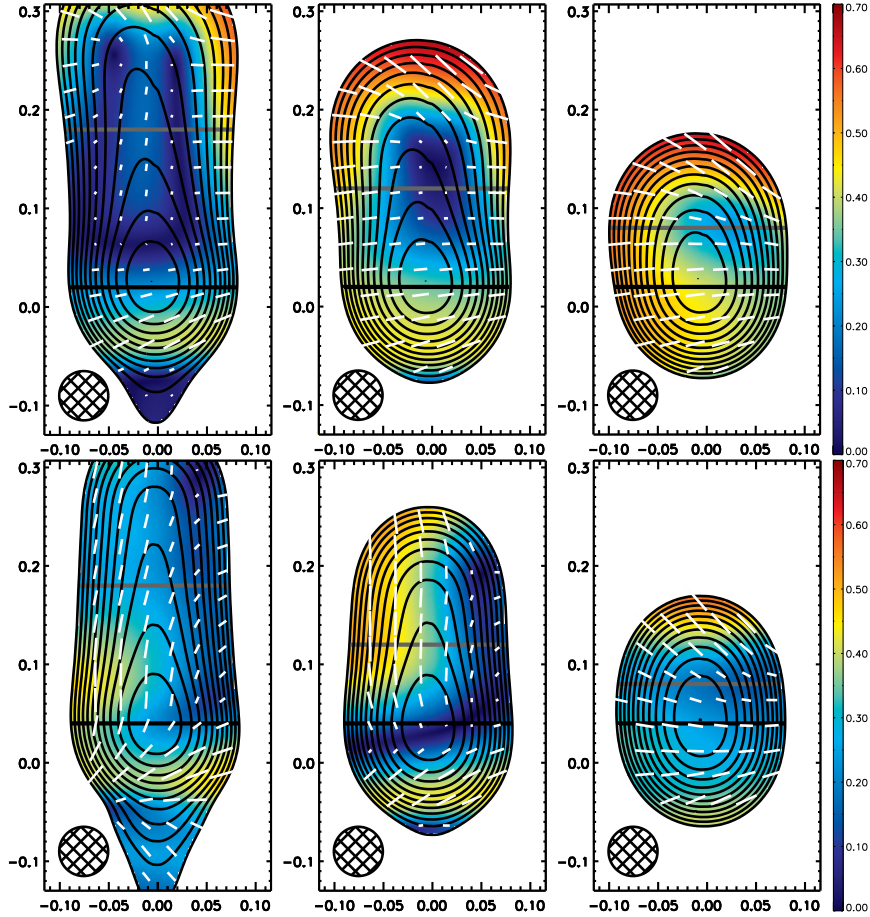


Fig. 3. Polarizations for inclination 30, 20, 10 degree (left to right) emitted from regions with comoving pitches $B'_\phi/B'_p > 1$ (above) and $B'_\phi/B'_p > 2$ (below). The polarization degree II43 GHz is color-coded, and intensity 43 GHz contours are shown. The spatial scale is given in milliarcseconds, and a restoring beam with FWHM = 0.05 mas was used. Figures taken from [17].

disk pressure distribution. This disk asymmetry leads first to disk warping and, subsequently, to asymmetric jet and counter jets differing in mass flux or velocity by about 30%. Depending on the magnetic diffusivity prescription (global model or local model), the jet - counter jet asymmetries are long lasting. We also observed a reversal of the asymmetry, meaning that the jet with high mass flux weakens and becomes less massive than the counter jet. The time scale for these reversals is about 1000 dynamical time scales of the inner disk. For AGN jets, the timescale for jet fluctuations corresponds to 2 yr, assuming an inner disk radius of 10 Schwarzschild radii and a central black hole mass of 10^8 solar masses. This is remarkably similar to the ejection times observed in e.g. 3C 120²³ or 3C 390.3²⁴.

6 Authors' Names

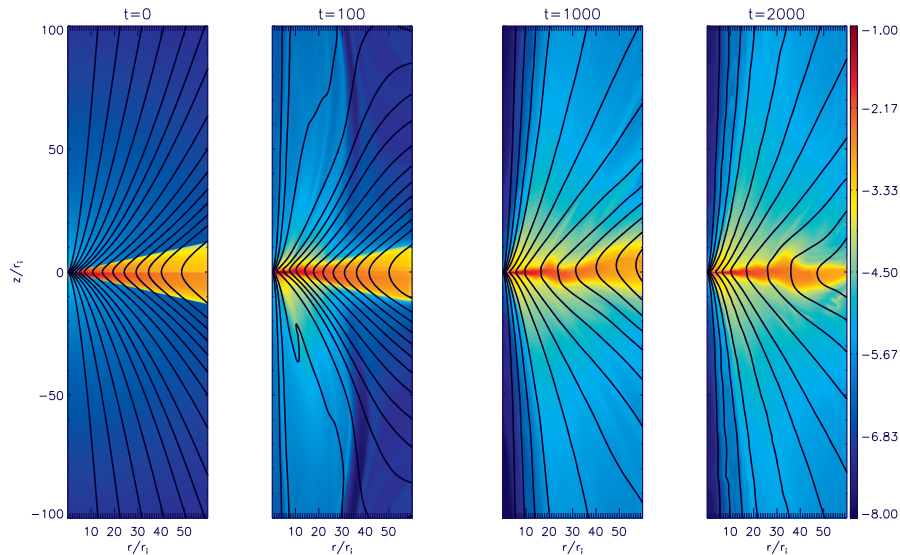


Fig. 4. Time evolution of the bipolar jet-disk structure for a simulation starting from an initial initial state with different thermal scale heights for the upper and lower disk hemispheres. Shown is the evolution for dynamical time $t = 0, 100, 1000, 2000$ of the mass density (colors) and the poloidal magnetic field (lines). Figures taken from [22].

Acknowledgments

This work was partly financed by the SFB 881 of DFG, project B4, and the IMPRS for Astronomy & Cosmic Physics at the University of Heidelberg. We thank Andrea Mignone for the possibility to use the PLUTO code. The simulations were performed on the THEO cluster of the Max Planck Institute for Astronomy.

References

1. Blandford, R.D. & Payne, D.G. *MNRAS* **199**, 883 (1982)
2. Pudritz, R.E., Ouyed, R., Fendt, Ch., Brandenburg, A. 2007, in: B. Reipurth, D. Jewitt, & K. Keil (eds.), *Protostars & Planets V*, U. of Arizona Press, Tucson, 2007, p.277
3. Shang, H., Li, Z.-Y., Hirano, N. 2007, in: B. Reipurth, D. Jewitt, & K. Keil (eds.), *Protostars & Planets V*, U. of Arizona Press, Tucson, 2007, p.261
4. Keppens, R., Goedbloed, J.P. *A&A* **343**, 351 (1999)
5. Matt, S., Pudritz, R.E. *ApJ* **678**, 1109 (2008)
6. Fendt, C. *ApJ* **692**, 346 (2009)
7. Blandford, R.D. & Znajek, R.L. *MNRAS* **179**, 433 (1977)
8. Tchekhovskoy, A., McKinney, J.C. *MNRAS* **423**, L55 (2012)
9. Fendt, C. *A&A* **319**, 1025 (1997)
10. Fendt, C. & Greiner, J. *A&A* **369**, 308 (2001)
11. Vlahakis, N. & Königl, A. *ApJ* **605**, 656 (2004)
12. Koide, S., Meier, D.L., Shibata, K., Kudoh, T. *ApJ* **536**, 668 (2000)

13. McKinney, J.C. *ApJ* **630**, 5 (2005)
14. Komissarov, S.S., Barkov, M.V., Vlahakis, N., Königl, A. *MNRAS* **380**, 51 (2007)
15. Mignone, A., Bodo, G., Massaglia, S., Matsakos, T., Tesileanu, O., Zanni, C., Ferrari, A. *ApJS* **170**, 22 (2007)
16. Porth, O., Fendt, C. *ApJ* **709**, 1100 (2010)
17. Porth, O., Fendt, C., Meliani, Z., Vaidya, B. *ApJ* **737**, 42 (2011)
18. Heyvaerts, J. & Norman, C. *ApJ*, **347**, 1055 (1989)
19. Chiueh, T., Li, Z.-Y., Begelman, M.C. *ApJ* **377**, 462 (1991)
20. Bucciantini, N., Del Zanna, L. *MNRAS* **428**, 71 (2013)
21. Sheikhezami, S., Fendt, C., Porth, O., Vaidya, B., Ghanbari, J., *ApJ* **757**, 65 (2012)
22. Fendt, C., Sheikhezami, S. *ApJ* **774**, 12 (2013)
23. Leon-Tavares, J., Lobanov, A.P., Chavushyan, V.H., Arshakian, T.G., Doroshenko, V.T., Sergeev, S.G., Efimov, Y.S., Nazarov, S.V. *ApJ* **715**, 355 (2010)
24. Arshakian, T.G., Leon-Tavares, J., Lobanov, A.P., Chavushyan, V.H., Shapovalova, A.I., Burenkov, A.N., Zensus, J.A. *MNRAS* **401**, 1231 (2010)